CONF-850713--7

DE85 016472

CONF-850713--7

DISCLAIMER

ABSTRACT

Because commercial liquid metal fast breeder reactors (LMFBRs) are designed to last for 40 years or more, an understanding of the mechanical behavior of the structural alloys used in them is required for times on the order of 2.5×10^5 h (assuming a 70% availability factor). Types 304 and 316 stainless steel are used extensively in LMFBR systems. At the beginning of life these alloys are in a metastable state and evolve to a more stable state and, therefore, more stable microstructure during plant operation. Correlations of microstructures and mechanical properties during aging under representative LMFBR temperature and loading conditions are desirable from the standpoint of assuring safe, reliable, and economic plant operation. We reviewed the mechanical properties and microstructures of types 304 and 316 stainless steel wrought alloys after long-term aging in air for times up to 9×10^4 h (about 10-1/2 years). The principal effect of such aging is to reduce low temperature fracture toughness (as measured by Charpy impact tests) and tensile ductility. Examples are cited, however, where, because stable microstructures are achieved, these as well as strength-related properties can be expected to remain adequate for anticipated service life conditions.

LONG-TERM AGING AT LMFBR operating temperatures results in changes in microstructures and associated mechanical properties of the structural alloys for LMFBRs. The changes in mechanical properties produced by aging can have a significant effect on the plant availability factor and reliability. To provide high availability and reliability, information on changes in mechanical properties produced by aging should be included early in the design process and in the plant operation, inspection, and maintenance criteria and schedules.

To ensure that a commercial LMFBR plant can meet its design objectives requires the capability to predict the behavior of structural alloys for times on the order of 2.5×10^5 h (assuming an availability factor of 70%). For this purpose, correlations between the microstructures and the mechanical properties of these alloys during aging under representative LMFBR temperatures and loading conditions are desirable. Such correlations are useful for extrapolating materials behavior to anticipated design lifetimes, interpolating materials behavior to conditions that are intermediate to those used in laboratory tests, predicting the response of components and structures to off-normal operating conditions, and providing the information necessary to scale up from laboratory test conditions and specimen sizes to full-size reactor components and structures.

Types 304 and 316 stainless steel are the major structural alloys used in LMFBR designs. These alloys are in a metastable thermodynamic state at the beginning of plant operation. During prolonged exposure to the temperatures and stresses of LMFBR operation, they evolve to more stable thermodynamic states and, therefore, microstructures. Weiss and Stickler described the thermodynamics and the microstructural changes that occur in type 316 stainless steel when the solid solution austenite is exposed to elevated temperatures for long times.[1]

This paper presents information generated in the U.S. Department of Energy LMFBR Materials and Structures Program on (a) the mechanical properties of types 304 and 316 stainless steel wrought alloys after long-term aging in air to 9×10^4 h (about 10-1/2 years) at temperatures in the range of

427 to 649°C (800 to 1200°F), after creep, and after fatigue deformation and
(b) microstructural evolution during long-term aging to 1.25×10^5 h (about 14 1/2 years) and testing for these alloys.

REVIEW AND DISCUSSION OF PROPERTIES AND MICROSTRUCTURES

TENSILE PROPERTIES - The effects of laboratory aging or service exposure to times of 5.1×10^4 h at temperatures to 649°C (1200°F) on the microstructure and tensile properties of mill-annealed type 316 stainless steel are shown in Fig. 1.[2] In the unaged condition the microstructure shows only high-angle grain boundaries. After 4.4×10^3 h (about 6 months) at 649°C (1200°F) (0.53 T_m for this alloy where T_m is the absolute melting temperature), large carbide particles are present on these boundaries. After 5.1×10^4 h (about 6 years) at this temperature, carbide precipitation has occurred within the grains as well as at the grain boundaries; carbon, chromium, nickel, and molybdenum originally in solid solution are found in the large particles shown in Fig. 1. The strength properties after aging are within the scatter band of these properties for unaged material.

Additional information on the effects of longer term aging on the tensile properties of type 316 stainless steel is contained in Figs. 2 and 3. The data in Fig. 1 are for only four aging times, but those in Figs. 2 and 3 are for 12 aging times.[3-9] For the important temperature range of application for this steel in LMFBRs [500–625°C (930–1160°F)], the 0.2% yield and ultimate tensile strengths are either unaffected or increased by aging. Thus, it is reasonable to state that no unforeseen decreases in strength will occur for unstressed material for service times between about 10 1/2 years (Figs. 2 and 3) and service lifetimes of approximately 28 years for commercial LMFBRs. For some of the times shown in Figs. 2 and 3, at temperatures above 550°C (1022°F) precipitation reactions are essentially complete for this alloy, and a stable matrix and grain-boundary structure should be present. For aging temperatures of 593°C (1100°F) and above the ductility falls below the minimum ductility measured on unaged material. However, total elongation and reduction of area are still above 20%, which is acceptable. Some implications of the lower ductility of aged material are discussed later under "TOUGHNESS PROPERTIES."

Knowledge of the effects of prior loading also is needed for extrapolation to conditions beyond laboratory tests. Prior loading can also be a form of aging; the effects of prior loading on the mechanical properties of structural alloys should be assessed in a methodology that attempts to assure high plant availability and reliability. Figures 4 and 5 contain data on the effects of prior creep and fatigue loading, respectively, on the tensile properties of type 304 stainless steel.[2,10] At 538 and 593°C (1000 and 1100°F), strength and ductility properties decrease linearly as a function of prior creep strain. Prior creep strain of 0.17 to 0.18 produces a 20% decrease in ultimate tensile strength but a much larger decrease in ductility, as shown by the 50% decrease in total elongation.

For these tests, cyclic loading at 593°C (1100°F) and a total strain range of 0.4% has no effect on the tensile properties of type 304 stainless steel at this temperature, even for cycling to 75% of the fatigue life (cycles to failure). For a total strain range of 1.0%, cyclic strengthening increases the yield strength by about 25%, the ductility decreases by about 25%, and the ultimate tensile strength is not affected. Adding tensile hold times of 0.1 and 0.5 h in each cycle at the 1% strain range has no further effect on the yield or ultimate tensile strength, but the ductility decreases with increasing hold time. At 75% of the fatigue life, the ductility (as measured by reduction of area) decreases almost 50% by a 0.1-h hold time, and at only 50% of the fatigue life the ductility is reduced by a 0.5-h hold time to only 43% of that before the creep-fatigue loading. This information indicates that continuous-cycling fatigue loading at maximum strain ranges to 1% at 593°C (1100°F) has little, if any, effect on the tensile properties of type 304 stainless steel. The data in Fig. 5, combined with the data shown in Fig. 4, illustrate that creep damage produced in either monotonic or cyclic loading is detrimental to tensile properties. The tensile property most affected by creep loading is ductility.

CREEP-RUPTURE PROPERTIES - Figure 6 shows the forms of $Cr_{23}C_6$ precipitate particles in type 304 stainless steel after a creep-rupture test lasting 6×10^4 h (about 7 years) at 593°C (1100°F) and 117 MPa (17 ksi).[11,12] The precipitate particles are large (50–100 nm across) and primarily rectangular. Figure 7 shows massive precipitates of sigma phase and fine precipitates of $Cr_{23}C_6$ in the same sample. Figure 8 shows that sufficient localized chromium depletion from the austenite during precipitation of sigma phase can result in the sigma phase particles being surrounded by ferrite.

Figure 9 is an optical micrograph from a creep-rupture specimen of type 304 stainless steel that ruptured after 7.3×10^4 h (about 8 1/2 years) at 593°C (1100°F) and 117 MPa (17 ksi). At the lower center of the micrograph is evidence that the original grain boundary moved during the test. The matrix in this area is apparently void of any precipitates. Apparently they were dissolved during

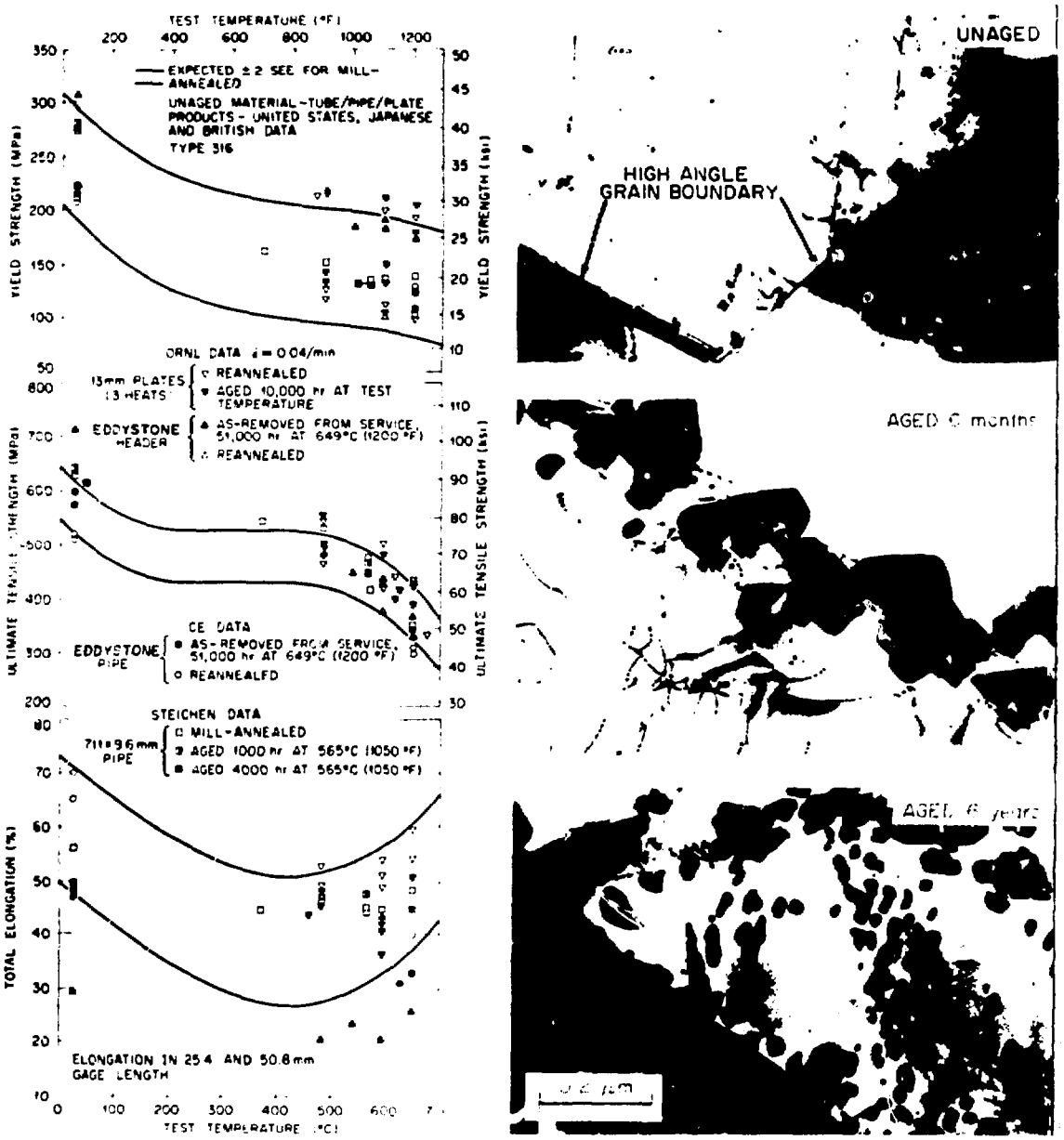

Fig. 1 – Tensile properties and microstructures of mill-annealed type 316 stainless steel aged for times to 5.1×10^4 h (about 6 years) and reannealed after the 10^4 h and 5.1×10^4 h aging conditions[2]

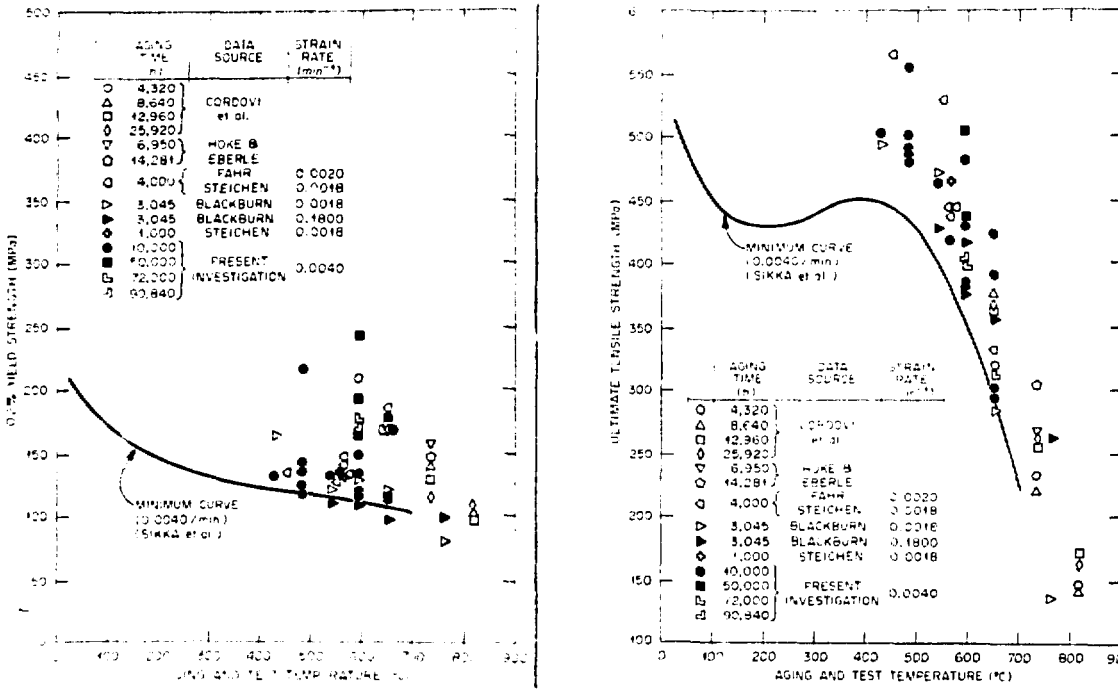

Fig. 2 - Yield and ultimate strengths of type 316 stainless steel in the annealed condition and after aging for times to 9.1 x 10^4 h (about 10 1/2 years)[3-9]

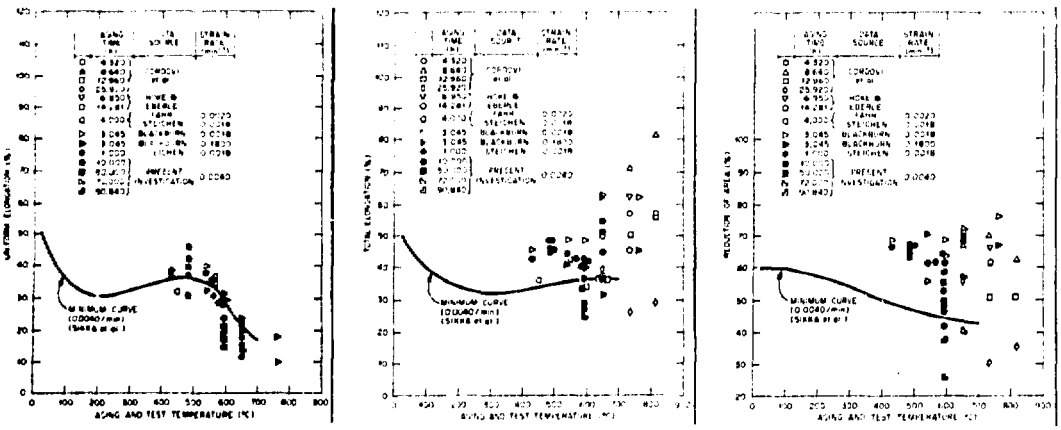

Fig. 3 - Uniform and total elongation and reduction of area of type 316 stainless steel in the annealed condition and after aging for times to 9.1 x 10^4 h (about 10 1/2 years)[3-9]

the grain-boundary movement under the applied stress. The grains contain an essentially uniform distribution of carbide particles, and massive sigma phase particles are found at grain-boundary intersections. The information derived from these figures shows that the time-temperature-precipitation diagrams developed by Stickler and Vinckier for type 304[13] and by Weiss and Stickler for type 316 stainless steel[1] can be very effectively used to predict the microstructures and associated mechanical properties of these alloys for long-term testing and service conditions in the operation of LMFBRs.

Figure 10 contains data for the creep-rupture life for 11 heats of type 304 stainless steel tested at 593°C (1100°F) and the minimum time-to-rupture curve as given in

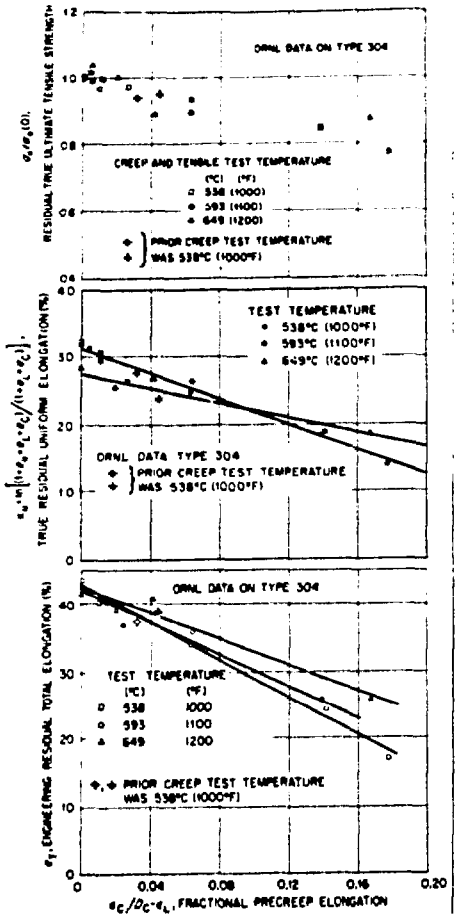

Fig. 4 - Residual tensile properties of type 304 stainless steel at 583, 593, and 649°C (1000, 1100, and 1200°F) as a function of prior creep elongation[2]
where

e_L = engineering loading strain,
e_C = engineering creep strain,
ϵ_C = true prior creep strain,
ϵ_L = true loading strain = ln $(1+e_L)$,
D_C = true creep ductility = ln (100/100 − RA),
RA = reduction of area (%)

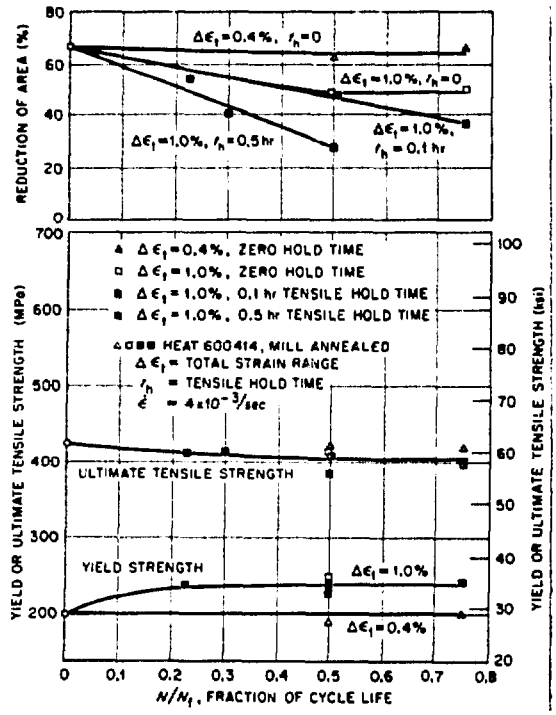

Fig. 5 - Tensile properties as a function of cycle life expended for type 304 stainless steel cycled in strain control at 593°C (1100°F) (N_f = cycles to failure)[10]

ASME Code Case N-47. Except for a few tests at 172 MPa (25 ksi), these results indicate that the long-term creep-rupture properties for type 304 stainless steel are well above the ASME minimum for rupture lives to 9.6×10^4 h (about 11 years).

Figure 11 shows the creep curves at 593°C (1100°F) and a stress of 172 MPa (25 ksi) for type 316 stainless steel in the annealed condition and after aging for 10^4 h (about 1 year) at 593°C (1100°F). This aging increases the secondary (steady-state) creep rate, the rupture life, the rupture ductility, and the time to onset of tertiary creep. The effects of a much longer aging time [4.4×10^4 h (about 5 years)] on the creep rupture

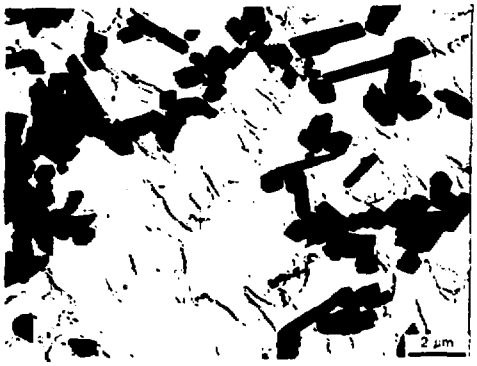

Fig. 6 – Transmission electron micrograph of carbon extraction replica showing forms of $Cr_{23}C_6$ particles extracted from the stressed region of type 304 stainless steel after 6×10^4 h (about 7 years) at 593°C (1100°F) and 117 MPa (17 ksi)[12]

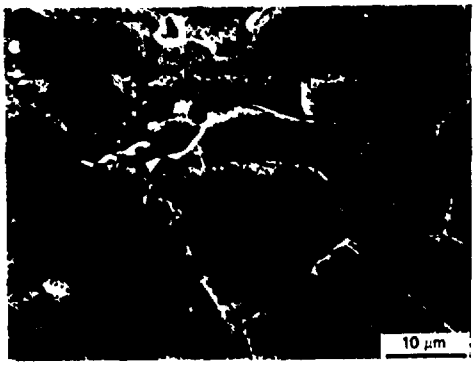

Fig. 7 – Scanning electron micrograph showing massive sigma phase and fine particles of $Cr_{23}C_6$ precipitated in the stressed region of type 304 stainless steel during 6×10^4 h (about 7 years) at 593°C (1100°F) and 117 MPa (17 ksi)[12]

curves for type 316 stainless steel at 593°C (1100°F) are shown in Fig. 12 for a stress of 207 MPa (30 ksi). At 172 MPa (25 ksi) (same stress as in Fig. 11) aging for 4.4×10^4 h (about 5 years) results in a large increase in secondary creep rate, a slight increase in ductility, and in a slight decrease in the times to the onset of tertiary creep and rupture. For the higher stress of 207 MPa (30 ksi) this aging results in a large increase in the secondary creep rate and ductility and in large decreases in the times to onset of tertiary creep and rupture. Note that aging increases creep ductility (low strain rates) but decreases tensile ductility (high strain rates).

Figure 13 shows stress versus time to rupture at 593°C (1100°F) for type 316 stainless steel annealed and after aging for times to 7.4×10^4 h (about 8 1/2 years) at temperatures from 482 to 649°C (900 to 1200°F). Also shown in Fig. 13 is the minimum stress versus time to rupture from ASME Code Case N-47. For all aging histories shown, the time to rupture for aged material exceeds that for the ASME minimum. Hence, long-term thermal exposures (~5 years) at temperatures up to 649°C (1200°F) and stresses too low to drastically alter the precipitation reactions do not shorten the subsequent creep-rupture life of type 316 stainless steel at temperatures to 593°C (1100°F). As stated for the tensile properties, little or no further effects of aging on the creep-rupture properties are expected as a result of additional thermal exposures at low stresses for temperatures to about 593°C (1100°F).[14]

Figures 14 and 11 show optical metallography for type 316 stainless steel after creep testing at 593°C (1100°F) and 172 MPa (25 ksi) in the annealed condition and after aging for 10^4 h (about 1 year) at 593°C

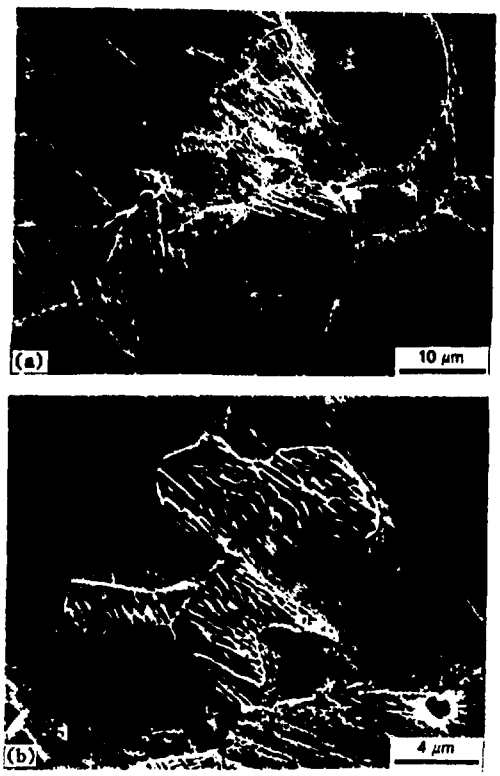

Fig. 8 – Scanning electron micrograph showing large islands of ferrite containing fine particles of sigma phase precipitated in the stressed region of type 304 stainless steel during 6×10^4 h (about 7 years) at 593°C (1100°F) and 117 MPA (17 ksi)[12]

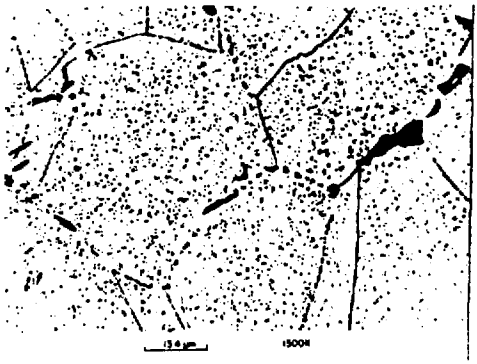

Fig. 9 - Optical micrograph showing large amounts of carbide precipitation within the matrix and large sigma phase particles at the grain boundaries in the stressed region of type 304 stainless steel during 7.3×10^4 h (about 8 1/2 years) at 593°C (1100°F) and 117 MPa (17 ksi)

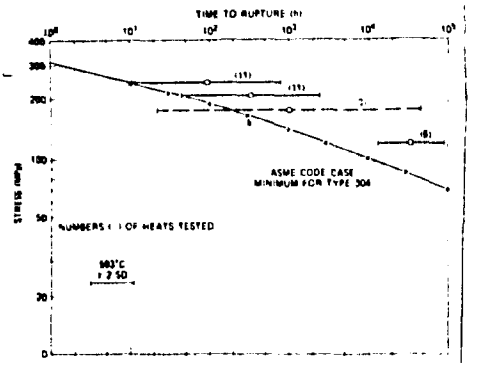

Fig. 10 - Stress-rupture properties at 593°C for 11 heats of type 304 stainless steel and ASME Code Case N-47 minimum for type 304 stainless steel at 593°C (1100°F)

(1100°F). In annealed material the applied stress results in considerable grain-boundary cavitation [Fig. 14(a)] and intergranular failure with little or no plastic deformation of the grains, but in aged material the same applied stress results in extensive plastic deformation of the grains and small ductile intragranular cavitation, leading to ductile tearing with no observable grain-boundary cavitation or intergranular failure [Fig. 14(b)]. The higher ductility and the associated benefits of the aged material compared with those of the annealed material are clearly evident in Fig. 14. Figure 11, which includes optical micrographs at a much higher magnification than those shown in Fig. 14, shows the details of the microstructure and mode of failure for the aged [Fig. 11(a)] and the annealed [Fig. 11(b)] materials. At this magnification, for the annealed material some precipitate particles are observed at the grain boundaries but none are observed within the grains. Intergranular cavitation and cracking are the dominant modes of failure. The aged material has many small precipitate particles at the grain boundaries and within the grains. For this microstructure, deformation of grains and nucleation of cracks at annealing twins has been observed to be the mode of deformation and failure.[15] Precipitation during aging has strengthened the grain boundaries relative to annealed material and has thereby eliminated intergranular cavitation and fracture, resulting in longer creep-rupture life.

Comparison of the microstructure shown in Figs. 11(a) and 12(a) indicate that the precipitate structure and deformation mode are the same for material aged for 10^4 h (about 1 year before testing and for material aged for 4.4×10^4 h (about 5 years) before testing. This provides further evidence that the aged structure is sufficiently stable for elevated-temperature applications in LMFBRs.

Figure 15 shows the sigma phase precipitate present in type 316 stainless steel after 1.25×10^5 h (about 14 1/2 years) of service at 621°C (1150°F) and is very consistent with the analysis of Weiss and Stickler.[2] Although this temperature is well above that anticipated for type 316 stainless steel for out-of-core applications, testing at lower temperatures must be continued to determine if similar structures will be produced by longer exposures at lower temperatures combined with LMFBR operating stresses.

As stated in the sections on tensile properties, prior loading is a form of aging for most structural alloys. The effect of fatigue loading prior to monotonic creep loading appears to be a function of the ratio of the applied stresses during the fatigue and creep portions of the testing. Samples of type 316 stainless steel were subjected at 593°C (1100°F) to 10^4 cycles with a total strain range ($\Delta\varepsilon_t$) of 0.20%, 10^2 and 10^3 cycles with a $\Delta\varepsilon_t$ of 0.40%, and 10^1 cycles with a $\Delta\varepsilon_t$ of 0.20, 0.40, 0.80, and 1.00% prior to creep testing at 593°C at a load of 207 MPa (30 ksi). Current emphasis is on material in which $\Delta\varepsilon_t$ was 0.20 and 0.40% since these strains are more relevant to LMFBR operating conditions than are the higher strains. For tests in which the ratio of applied stress during creep testing, σ_c, to the half-cycle stress during fatigue testing, $\sigma_{f/2}$, is greater than unity, $\sigma_c/\sigma_{f/2} > 1$, the minimum creep rate, $\dot{\varepsilon}_{min}$, is lower than for material with no fatigue loading prior to creep testing. This effect is attributed to cyclic strain strengthening and precipitation strengthening during the fatigue portions of the test. For tests in which $\sigma_c/\sigma_{f/2} < 1$, $\dot{\varepsilon}_{min}$ is the same as that for material with no fatigue loading prior to creep testing. However, for these tests the primary creep strain, ε_p,

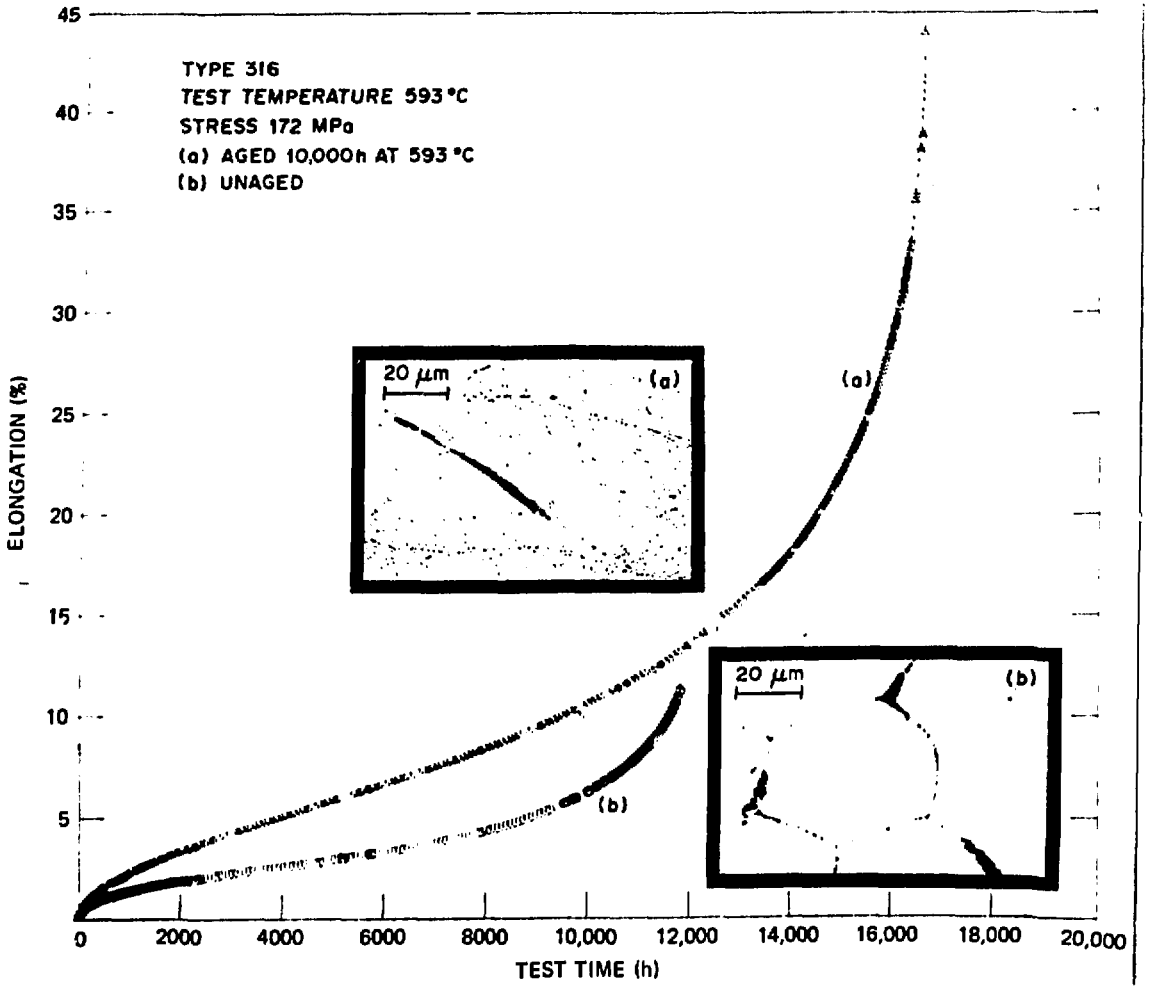

Fig. 11 - Elongation as a function of test time at 593°C (1100°F) and 172 MPa (25 ksi) and optical microstructures for type 316 stainless steel annealed and after aging for 10^4 h (about 1 year). The micrographs show (a) fine precipitate structure, intragranular deformation, and annealing twin cracks in aged materials and (b) lack of grain deformation and intergranular cracks in annealed material

is larger which results in higher total strains than for uncycled material. Therefore, within the range of loading conditions employed in these tests, cyclic loading prior to creep loading does not appear to adversely affect the creep properties of type 316 stainless steel at 593°C, and such loading should not affect the availability and/or reliability of LMFBRs.

FATIGUE AND CREEP-FATIGUE PROPERTIES - Figures 16 through 18 show the effects of relatively short-term aging on the cyclic creep-fatigue lifetimes and microstructures of type 316 stainless steel tested at 550°C (1022°F). All three figures show the same plots of strain range versus fatigue life; however, each of these figures shows a different and important aspect of the

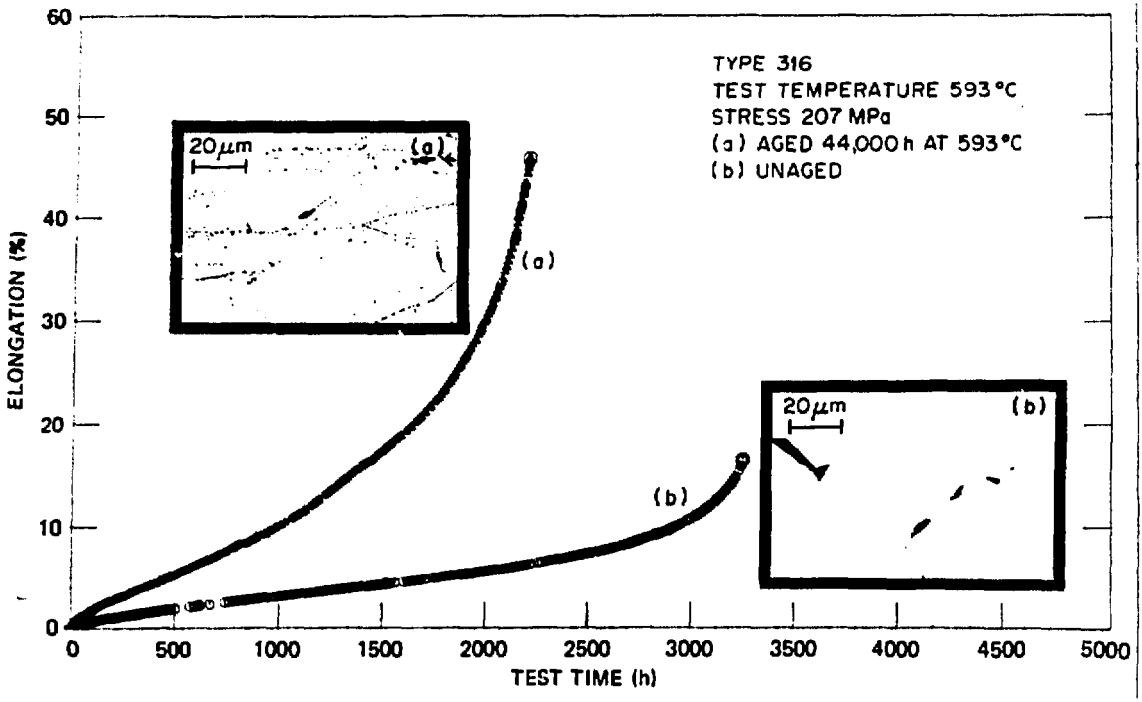

Fig. 12 - Elongation as a function of test time at 593°C (1100°F) and 207 MPa (30 ksi) and optical microstructures for type 316 stainless steel annealed and after aging for 4.4×10^4 h (about 5 years)

microstructures associated with the different fatigue curves. The dashed curve is for continuous cycling. For annealed material (curve a) a tensile hold period of 0.5 h during each cycle reduces the creep-fatigue life to only one-fourth that for continuous cycling. Aging for 10^3 h (about 1 month) at 593°C (1100°F) (curve b) improves the creep-fatigue life to approximately two-thirds of that for continuous cycling. Aging for 2×10^3 h (about 3 months) at 750°C (1382°F) (curve c) improves the creep-fatigue life to almost 25% greater than that for continuous cycling and more than 4 times that for unaged material under the same test conditions. Aging also improves the continuous-cycling fatigue life, but the magnitude of the improvement is not as great as that for the creep-fatigue life.

The microstructure is shown by optical microscopy in Fig. 16. The annealed material (a) shows a small amount of precipitation ($M_{23}C_6$) at the grain boundaries and very little observable precipitation within the grains. In (b) more precipitation occurs at the grain boundaries, and precipitation is observable at annealing twin boundaries and other sites within the grains. In (c) more massive precipitation is seen at the grain boundaries and within the grains, and the intragranular precipitate particles appear to be larger than in (b). Figure 17 shows scanning electron microscopy for material having the creep-fatigue lives shown by curves a, b, and c. The amount of grain-boundary precipitate increases by large increments during aging, as shown in micrographs (a), (b), and (c). Data trends in Fig. 17 clearly show that the increase in creep-fatigue life on aging is due to the alteration of the grain-boundary and matrix structure by precipitation.

Figure 18 shows scanning electron fractography associated with creep-fatigue curves (a), (b), and (c). For annealed material (a) fracture is intergranular with some ductile tearing. For (b) some intergranular failure is combined with an increased amount of ductile tearing. In (c) the fractograph indicates that failure was totally by intragranular ductile tearing, with no evidence of brittle intergranular failure. As discussed earlier, alteration of the grain-boundary and matrix microstructure by these precipitates reduces or eliminates grain-boundary cavitation and cracking during creep loading and thereby improves the creep-rupture and creep-fatigue properties.

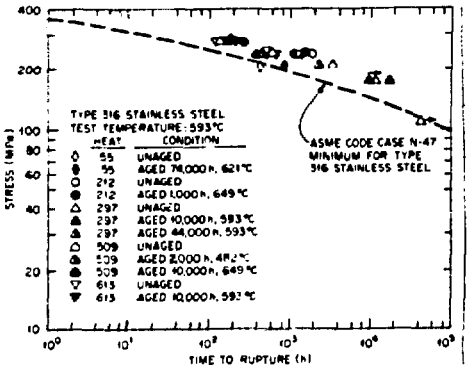

Fig. 13 - Stress-rupture properties at 593°C (1100°F) for type 316 stainless steel annealed and after aging to 7.4×10^4 h (about 8 1/2 years) and ASME Code Case N-47 minimum for type 316 stainless steel at 593°C (1100°F)

Fig. 14 - Fracture behavior of type 316 stainless steel creep-rupture tested at 593°C (1100°F) and 172 MPa (25 ksi). (a) Annealed; extensive intergranular cracking with large cavities and no intragranular deformation. (b) Aged for 10^4 h (about 1 year) at 593°C (1100°F); considerable intragranular deformation with few small- to medium-size cavities

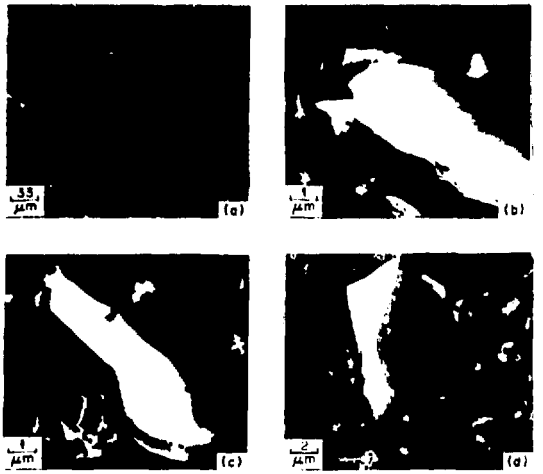

Fig. 15 - Scanning electron micrographs of type 316 stainless steel pipe after 1.25×10^5 h (about 14 1/2 years) of service at 621°C (1150°F). (a) Overview. (b) Laminated structure of large sigma phase particles in the grain boundaries of (a). (c) Delamination of sigma phase particles and matrix precipitate. (d) Delamination of another sigma phase particle and additional matrix precipitate[11]

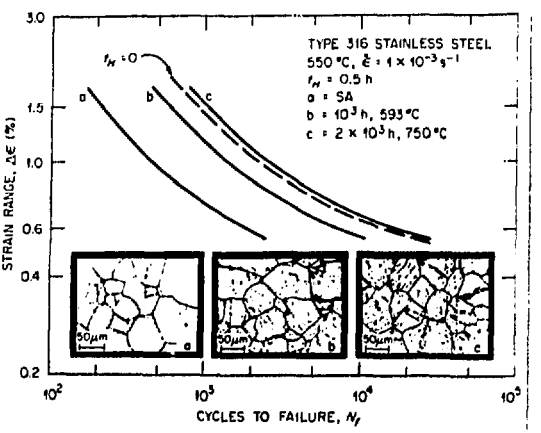

Fig. 16 - Strain range versus cycles to failure for cyclic creep-fatigue of type 316 stainless steel at 550°C (1022°F) and optical micrographs for material (a) as annealed, (b) aged for 10^3 h (about 1 month) at 593°C (1100°F), and (c) aged for 2×10^3 h (about 3 months) at 750°C (1382°F). Dashed line is for continuous cycling fatigue with no hold time; solid lines for cyclic creep-fatigue with 0.5 h tensile hold time.

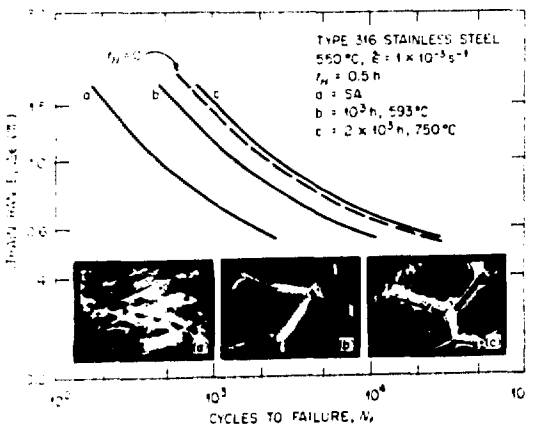

Fig. 17 - Strain range versus cycles to failure for cyclic creep-fatigue of type 316 stainless steel at 550°C (1022°F) and scanning electron micrographs for material (a) as annealed, (b) aged for 10^3 h (about 1 month) at 593°C (1100°F), and (c) aged for 2 x 10^3 h (about 3 months) at 750°C (1382°F). Dashed line is for continuous cycling fatigue with no hold time; solid lines for cyclic creep fatigue with 0.5 h tensile hold time

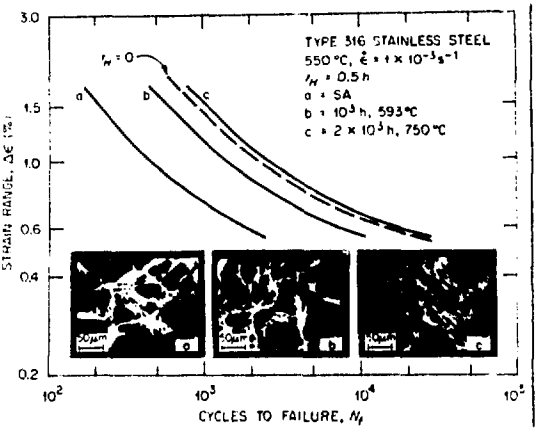

Fig. 18 - Strain range versus cycles to failure for cyclic creep-fatigue of type 316 stainless steel at 550°C (1022°F) and scanning electron fractographs for material (a) as annealed, (b) aged for 10^3 h (about 1 month) at 593°C (1100°F), and (c) aged for 2 x 10^3 h (about 3 months) at 750°C (1382°F). Dashed line is for continuous cycling fatigue with no hold time; solid lines for cyclic creep-fatigue with 0.5 h tensile hold time

TOUGHNESS PROPERTIES - The Charpy impact properties of austenitic stainless steels are not measured or cited very often because austenitic stainless steels normally do not lose fracture toughness or change from ductile to brittle behavior at low temperatures. However, as shown in Fig. 19(a), prolonged elevated-temperature exposure of type 316 stainless steel can result in room-temperature Charpy impact energies that are less than 10% of that for material in the annealed and unaged condition. Data in Fig. 19(a) are for both laboratory test specimens and material taken from actual power plant components.

Recall that, as shown in Figs. 1 through 5, tensile ductility is the property that is affected most by prior creep or fatigue loading or by thermal exposure for type 316 stainless steel. This decrease in tensile ductility is further manifested in the Charpy impact energy values. Charpy impact energy values for type 316 stainless steel weldments with type 16-8-2 weld alloy agree reasonably well with those for base metal, as shown in Fig. 19(b). For the time, temperature, and stress conditions shown in Fig. 19(b), the Charpy impact properties of the weld metals are superior to those of the base metal.

Work is in progress to attempt to relate the room-temperature Charpy impact properties with the elevated-temperature slower strain rate properties of these materials. This is not considered to be a concern for LMFBR systems because room-temperature Charpy impact values exaggerate the decrease in elevated-temperature toughness on aging and because during operation LMFBR systems are not exposed to temperatures below about 205°C (400°F) (i.e., during refueling).

SUMMARY

The information presented in this paper supports the following conclusions:

- The long-term mechanical properties of types 304 and 316 stainless steel can be correlated with the microstructures that are produced during elevated-temperature testing and/or service exposure relevant to LMFBR application.
- Long-term aging to 9.1 x 10^4 h (about 10 1/2 years) at temperatures to about 600°C (1100°F) has no detrimental effect on the tensile strength of type 316 stainless steel.
- Long-term aging to 9.1 x 10^4 h (about 10 1/2 years) at temperatures to about 600°C (1100°F) decreases the ductility of type 316 stainless steel; however, after 9.1 x 10^4 h at 649°C the ductility is still adequate for any anticipated out-of-core applications.
- Creep loading before tensile loading reduces the tensile properties of type 304 stainless steel.
- Fatigue loading before tensile loading has no effect on the tensile properties of type 304 stainless steel, but cyclic creep-fatigue loading reduces tensile ductility.

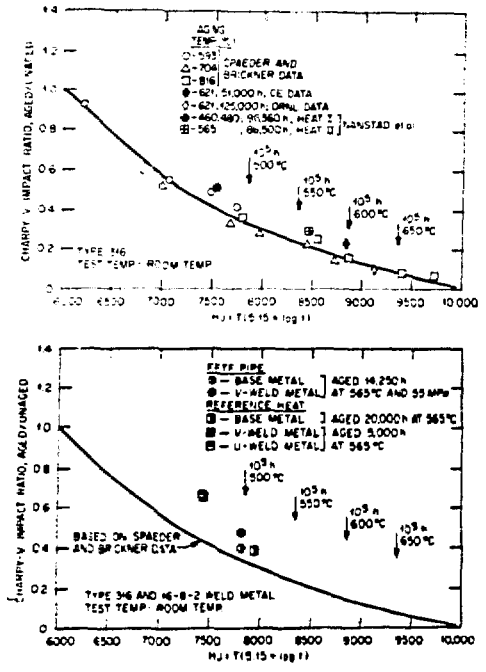

Fig. 19 - Room-temperature Charpy impact energy as a function of Holloman-Jaffe parameter for (a) type 316 stainless steel after thermal aging or in-service exposure and (b) curve for base metal and data for 16-8-2 weld metal after aging for up to 2×10^4 h (about 2 1/4 years) at 565°C (1050°F). (Ref. 7 and unpublished data from tests performed by ORNL and Combustion Engineering, Inc.) (T = test temperature and t = test time)

- For long-term testing and aging [~9.6×10^4 h (about 11 years)] of types 304 and 316 stainless steel, the stress-rupture properties exceed the minimum given in ASME Code Case N-47.
- For type 316 stainless steel, the precipitate structure produced by aging before creep loading increases the steady state creep rate and creep ductility and may slightly increase the time to rupture.
- Fatigue loading prior to creep loading has either no affect on minimum creep rate or results in slightly lower creep rates in type 316 stainless steel depending on the ratio of the stress applied during the fatigue and creep portions of the load history.
- Short-term (about 1 to 3 months) aging increases the fatigue life and creep-fatigue life of type 316 stainless steel by strengthening the grain boundaries.
- The precipitate structures that form during long-term aging or service exposure at elevated temperature decrease the room-temperature Charpy impact values of type 316 stainless steel and its weldments with type 16-8-2 filler metal.
- Long-term aging to 1.25×10^5 h (about 14 1/2 years) produces $M_{23}(C,N)_6$, sigma phase, and ferrite in types 304 and 316 stainless steel consistent with the time-temperature-precipitate diagrams of Weiss and Stickler;[1] therefore, the Weiss and Stickler diagrams may be used to predict long-term behavior of these alloys for LMFBR service.
- The mechanical properties of types 304 and 316 stainless steel appear to be satisfactory for the temperature and load conditions anticipated for the design lifetimes of commercial LMFBR out-of-core structures and components. The observed changes in mechanical properties of these structural alloys should not affect plant availabilty and/or reliability.

ACKNOWLEDGMENTS

The authors wish to express their appreciation to R. W. Swindeman and M. L. Grossbeck for reviewing this paper and to Donna Amburn for preparing many of the figures.

REFERENCES

1. B. Weiss and R. Stickler, Metall. Trans. 3, 851–66 (April 1972).
2. C. R. Brinkman, V. K. Sikka, and R. T. King, Nucl. Technol. 33, 76–97 (1977).
3. M. A. Cordovi, "Behavior of Superheater Alloys in High Temperature, High Pressure Steam", pp. 8–55, American Society of Mechanical Engineers, New York (1968).
4. J. Hoke and F. Eberle, Trans. ASME 79, 307–17 (1957).
5. L. D. Blackburn, Hanford Engineering Development Laboratory, Richland, Washington, private communication to V. K. Sikka, Oak Ridge National Laboratory, Oak Ridge, Tennessee, 1975.
6. J. M. Steichen, "Mechanical Properties of FFTF Primary Outlet Piping", HEDL-TME-75-15, Hanford Engineering Development Laboratory, Richland, Washington (January 1975).
7. D. Fahr, "Analysis of Stress-Strain Behavior of Type 316 Stainless Steel", ORNL/TM-4292, Oak Ridge National Laboratory, Oak Ridge, Tennessee (November 1973).

8. V. K. Sikka, C. R. Brinkman, and H. E. McCoy, Jr., "Structural Materials for Service at Elevated Temperatures in Nuclear Power Generation", pp. 316–50, The American Society of Mechanical Engineers, New York (1975).
9. V. K. Sikka, "Ductility and Toughness Considerations in Elevated Temperature Service", pp. 129–48, The American Society of Mechanical Engineers, New York (1978).
10. V. K. Sikka and C. R. Brinkman, "Proc. 2nd Int. Conf. Mechanical Behavior of Materials", American Society for Metals, Metals Park, Ohio (1976).
11. R. W. Swindeman, V. K. Sikka, and R. L. Klueh, Metall. Trans. A 14A, 581–93 (April 1983).
12. V. A. Biss and V. K. Sikka, "Metallographic Study of Type 304 Stainless Steel Long-Term Creep-Rupture Specimen", ORNL/TM-7168, Oak Ridge National Laboratory, Oak Ridge, Tennessee (January 1981).
13. R. Stickler and A. Vinckier, ASM Trans. Q. 54, 362–80 (1961).
14. C. F. Etinne, W. Dortland, and H. B. Zeedijk, Int. Conf. Creep Fatigue in Elevated Temperature Applications 1, (1975).
15. F. G. Wilson, J. Iron Steel Inst. (London) 209, 126–30 (1971).
16. C. E. Spaeder, Jr., and K. G. Brickner, "Advances in the Technology of Stainless Steels and Related Alloys", pp. 143–50, American Society for Testing and Materials, Philadelphia, Pennsylvania (1963).